Simple Sound Speed Measurement Method for Liquids and Castable Phantom Materials

Wanwei Yu(余婉薇) and Nelson G. Chen(陳稷康)

***Abstract*— The speed of sound *c* is an important property of materials and fluids. Ultrasonic imaging is based on the assumed values of *c*, and the characterization of various phantom materials includes measurements of their *c* values. Measurements of *c*, to date, have required specialized setups that are not always readily available. The development of a simple alternative allows laboratories to measure *c* with a minimum of specialized equipment. In this article, a method using only a polypropylene (or other plastic) test tube, fishing line, a level, a sewing or suture needle, sodium chloride, and a conventional ultrasonic B-mode imager is described that allows one to measure *c* readily. The measurement is based on the difference between the apparent and actual distances separating two fishing line targets embedded within a test tube. The liquid or gel being measured is poured into the test tube and B-mode ultrasonic images are obtained using a conventional clinical imager. This method was tested on seven samples of saline solutions with varying salt concentrations, pure ethanol, and a tissue-mimicking gel to verify its accuracy over a broad range (1144–1700 m/s) of reference values. Sound speed measurements were, on average, 100.4% ± 0.86% of published values. No single measurement had a deviation exceeding 2.4%. The measurement of sound speed is simplified and may be accurately performed with minimal equipment.**

***Index Terms*— Biomedical imaging phantoms, biomedical materials, materials testing, ultrasonic imaging, ultrasonic variables measurement.**

I. Introduction

SOUND speed is a fundamental attribute of solids and liquids. Ultrasonic imaging, based on the pulse-echo technique, uses the sound speed to determine the location of interfaces. For biological tissue, an average value of 1540 m/s is assumed [1], even though the actual value varies depending on the tissue type. The differences in actual tissue from this value are known to cause image blurring [2] and cause parts of images to be displaced [1]. Sound speed is also relevant in other contexts; for instance, microbead and liquid cell suspensions of human red, white, and various cancer cells can be characterized using such [3]. Microalgal suspensions can also be characterized by their sound speed [4]. Sound speed can also be used to characterize nanofluids, namely, fluids containing suspended solid nanoparticles [5], [6]. Nanofluids containing different numbers and sizes of nanoparticles have different sound speeds, and this information has been used in ultrasonic spectroscopy to measure the concentration and size of suspended particles [7].

Tissue-mimicking phantom materials are designed to have properties approximating that of actual tissue. They include the proprietary hydrogel Zerdine, agarose [8], polyacrylamide [9], and rubber [10]. A critical parameter that needs to be measured regarding these materials is their sound speed. For instance, rubber phantoms have the advantage of being stable and durable over time but have a sound speed of less than 1540 m/s [2], [10]. When modifications are made to these materials through changing the additives present, sound speed may also be affected. Characterizing the materials as changes are made requires measuring the sound speed post-modification.

The existing methods of sound speed measurement use a variety of techniques. Pellam and Galt [11] developed a technique based on the transmission of a pulse that traverses the sample and is then reflected. An insertion technique that is commonly used examines the time-of-flight to a reflector and back with and without a solid sample present [12]. That technique requires a large bath within which the sample is suspended. The coagulation of milk has been monitored using a similar setup [13]. The use of two different coupling fluids for solids avoids issues with obtaining echoes from sample surfaces [14]. Ophir and Lin [15] developed a method for biological samples of unknown thickness where the samples are insonated with a receiving hydrophone stepped at known relative distances. These techniques require the construction of setups linking oscilloscopes, ultrasonic transducers, function generators, amplifiers, and possibly plate reflectors.

Examples of dedicated systems for measuring sound speed include those developed for monitoring the fermentation of wine [16]. Another system [17] uses two dedicated transducers that attach to a glass bottle holding biological samples to perform measurements while keeping sample disturbance to a minimum. The Acoustiscan system [18] uses stepper motors to adjust dedicated transducers to monitor colloids and other suspensions over time.

We report a simple alternative method of sound speed measurement that does not require any equipment other than

Manuscript received April 20, 2020; accepted August 27, 2020. Date of publication September 7, 2020; date of current version November 24, 2020. This work was supported in part by the Ministry of Science and Technology (Taiwan) under Grant MOST105-2221-E-009-094 and in part by National Chiao Tung University under Grant 108W205. The Associate Editor coordinating the review process was Dr. V. R. Singh. *(Corresponding author: Nelson G. Chen.)*

Wanwei Yu is with the Institute of Biomedical Engineering, National Chiao Tung University, Hsinchu 30010, Taiwan (e-mail: wwyuavery@gmail.com).

Nelson G. Chen is with the Department of Electrical and Computer Engineering, National Chiao Tung University, Hsinchu 30010, Taiwan (e-mail: ngchen@nctu.edu.tw).

Digital Object Identifier 10.1109/TIM.2020.3022136

a traditional or portable B-mode ultrasonic imager. The B-mode ultrasonic imager provides a convenient platform that already incorporates transducer, amplifier, function generator, and oscilloscope functions into a commercially available package. No setup beyond a one-time test tube construction and calibration is required, thereby simplifying the measurement process. The only other required items are a plastic test tube, fishing line, a level, a sewing or surgical needle, and waterproof liquid adhesive. Calibration furthermore requires sodium chloride. Ultrasonic B-mode imagers are becoming less expensive over time and could soon become ubiquitous in regular medical clinics [19]. A device has been reported [20] that has a production cost of around US $100 [21]. It is well-known that fishing line diameters are less than the typical spatial pulse lengths of around 0.3–1 mm [22], and that fishing line, therefore, forms excellent line targets. (Pulse length L is given by Nc/f, where N is the number of wavelengths composing a pulse, c the speed of sound, and f the frequency of the wave. For an extreme case of $N = 1$, $c = c_0 = 1540$ m/s, and $f = 10$ MHz, L is 154 μm which is still substantially longer than the 90-μm fishing line diameter used.) Each line appears on the image with a thickness approximately equal to the axial pulse length.

II. Materials and Methods

A. Theory

1) Principle of Measurement: Given a single line target located at a distance d from an imaging transducer, and an assumed sound speed $c_0 = 1540$ m/s that is equal to the actual sound speed of the medium, then $d = c_0 t/2$, where t is the round-trip pulse travel time for $c = c_0$. Solving for t, $t = 2d/c_0$. Now if the actual sound speed of the medium is $c = c_0 + \Delta c$, the round-trip travel time becomes $t' = 2d/c = 2d/(c_0 + \Delta c)$. (The term Δc may be positive or negative.) The value t' then corresponds to an apparent distance $d' = c_0 t'/2$ on the ultrasonic image, due to the imager assuming $c_0 = 1540$ m/s. Substituting for t' in the previous expression then gives $d' = c_0 d/(c_0 + \Delta c)$. The relationship between d and d' allows one to compute Δc. If there are two separate line targets, they each will have their own apparent and actual distances. The relationship between the apparent and actual distances is illustrated in Fig. 1.

Using two separate line targets avoids the difficulty in measuring d from the transducer face, as depicted in Fig. 2. For a single line target, the distance d from the transducer face can be affected by the transducer curvature. It also differs from measurement to measurement depending on how the operator positions the transducer; any vertical variation in positioning will alter d. Having two line targets and examining the distance $d_2 - d_1$ between them avoids issues with the absolute distance since effects equally affect both of the line targets. Liquids are measured by filling the test tube to the level of the transducer face; castable solids are cast into the test tube to a level covering both line targets. For solids, a liquid coupling agent, typically water, is next added to fill the test tube to the transducer face. Effects arising from the sound speed of the coupling agent are avoided since the coupling agent equally affects both of the line targets.

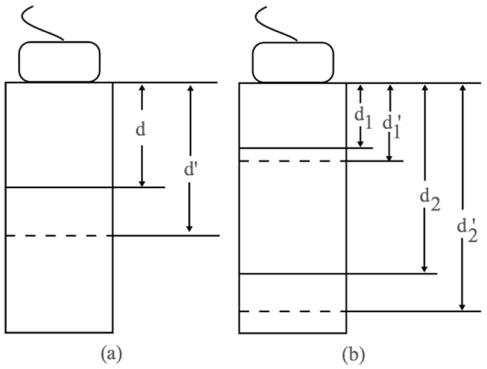

Fig. 1. Principle of measurement. (a) Given a line target located at an actual distance d from the transducer surface, the line target will appear to be located at a distance d' in a B-mode image due to the medium sound speed being different from $c_0 = 1540$ m/s. (b) Same principle can be applied to a pair of lines, providing, respectively, apparent and actual distance differences $d_2' - d_1'$ and $d_2 - d_1$.

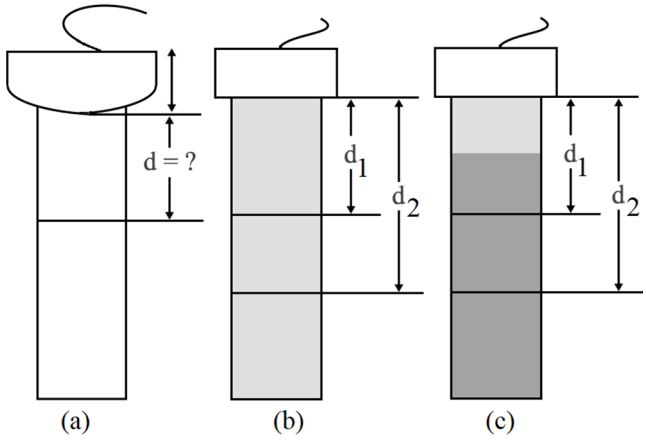

Fig. 2. Avoidance of absolute distance from transducer and measurement process. (a) Distance d for a single line target is variable. (b) Liquids are measured by filling the test tube to the transducer face. (c) For a solid material, denoted in dark gray, the measurement is made with a liquid coupling agent that is depicted in light gray.

With two line targets located at distances d_1 and d_2 from the transducer, their apparent distances d_1' and d_2' are, respectively, $d_1' = c_0 d_1/(c_0 + \Delta c)$ and $d_2' = c_0 d_2/(c_0 + \Delta c)$. The apparent distance between them $d_2' - d_1'$ is $c_0(d_2 - d_1)/(c_0 + \Delta c)$. Solving for Δc provides the following

$$\Delta c = c_0 \left(\frac{d_2 - d_1}{d_2' - d_1'} - 1 \right). \tag{1}$$

So for a pair of line targets with a known physical separation distance $d_2 - d_1$, and an apparent separation distance $d_2' - d_1'$ on an ultrasonic image, the actual difference in the medium sound speed from $c_0 = 1540$ m/s can be computed.

2) Effects of Deviations From Assumptions: In practice, examination of the ultrasonic images obtained would readily indicate any substantial deviation from the assumption of parallel line targets. The analysis below examines the effect of the line targets being inclined and being imperfectly parallel

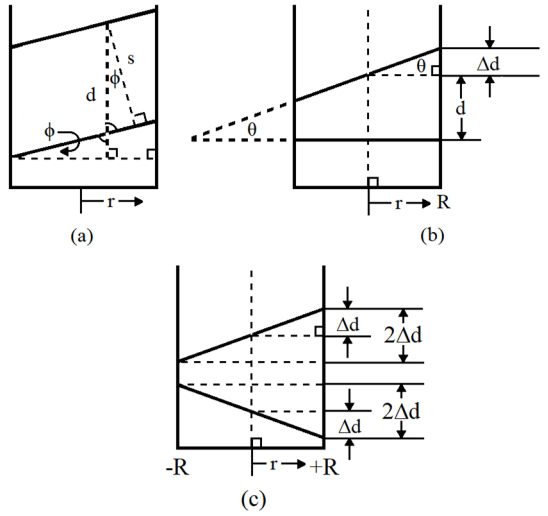

Fig. 3. Effect of deviations from assumptions (shown exaggerated). (a) If the lines were both inclined at a constant angle ϕ, such that they remain parallel, the vertical distance d remains unchanged for all r. (b) If the lines are not perfectly parallel, they will intersect at an angle θ. Nominal vertical distances become $d + r \tan \theta$. (c) Largest possible theoretical error of $4\Delta d$ occurs when the two distance measurements are taken at values $r = \pm R$, and both the lines are exactly inclined at opposite angles.

on the measured distances d. Factors that affect the resulting errors are identified together with their typical values to facilitate their minimization in tube selection and construction.

If the line targets were perfectly parallel, but both inclined at a fixed angle ϕ relative to the horizontal, the distance measurements d of the vertical segment separating the targets would become the constant s/cos ϕ, with s being the perpendicular distance between the lines. The targets being parallel means that measurements taken from different lateral locations r will not differ, as shown in Fig. 3(a). Were the transducer positioned such that its center beam was not vertical, the effect would be the same as having the parallel line targets inclined.

If the line targets are not perfectly parallel, then they will have an intersecting point if they were extended in space. (Were the lines skew lines, i.e., not both found within the same imaging plane, the anomalous geometry would be apparent upon imaging.) At this point of intersection, the lines form an angle θ. If one line is inclined by Δd at distance R from the centerline, then the angle θ is equal to $\tan^{-1}(\Delta d/R)$. The actual vertical separation distance between the lines then varies depending on the lateral location r. The distances measured at different lateral locations become different, with an amount $r \tan \theta$ added to d. (The term r can be positive or negative.) If both of the lines were inclined, they would simply form a different θ and the analysis remains valid.

The nominal line separation d affects the fractional errors caused by the lines being imperfectly parallel. The term Δd is expected to be nearly constant for any given phantom construction technique. Selecting large values of d minimizes the relative errors $\Delta d/d$ arising from nonparallelity. Also, making distance measurements near a constant reference point (e.g., near the image center) minimizes r and thereby also minimizes errors. Finally, having a larger R reduces θ for any given Δd and makes the lines more nearly parallel. These items are illustrated in Fig. 3(b). The maximum possible error is $4\Delta d$, obtained when the lines are inclined by the same amount in exactly opposite directions and distance measurements taken at the extremes of $\pm R$, as shown in Fig. 3(c). In practice, such an extreme situation is unlikely. Each term and its approximate value are listed in Table I.

TABLE I
VALUES OF TERMS

Symbol	Quantity	Value in practice
ϕ	angle at which parallel line targets are inclined	≈ 0
d, s	vertical and separation distance between targets, respectively	selected during construction, ideally large yet such that both targets will nonetheless appear in the image for the item being measured, usually several cm
R	test tube radius	~9-15 mm
r	horizontal (lateral) distance difference between the calibration and actual measurements	ideally 0, in practice a fraction no more than around 25% of *R*
Δd	half of the difference in vertical position between the left and right sides of a line target	ideally 0, in practice dependent on care in construction, $\Delta d \approx 0.5$ mm [a], note that $\Delta d << d$
θ	angle at which line targets intersect within plane	ideally 0 for perfectly parallel lines, in practice between 0 to 3-4° [b]
r tan θ	error in distance measurement arising from geometry	varies, normally no more than ~0.3 mm [c]

Approximate values in practice for items listed in Fig. 3.
[a]This figure is based on visual marking of the water level adjacent to the tube wall being accurate to within 1 mm.
[b]Estimated for values of *R* and Δd stated above for two independent lines, $\theta = \tan^{-1}(2\Delta d/2R) = \tan^{-1}(\Delta d/R)$ for one line. For two lines, Δd is increased on average by a factor of $\sqrt{2}$ [23].
[c]Note how this value is approximately the spatial pulse length of a transducer.

B. Experiments

1) Construction of Dual-Line Target Test Tube: An empty polypropylene centrifuge test tube (50 mL, self-standing, CFT111500, Guangzhou Jet Bio-Filtration Co. Ltd., Guangzhou, China) first was filled with water to a preselected level to provide a visual indication of a fixed distance from the top edge. Its radius R was approximately 14 mm. A level (EbisuDiamond Aluminum Super Level ED-10HLR, Ebisu Co. Ltd., Niigata, Japan) was used to verify that the top edge was horizontal. A sewing needle was threaded with a piece of 90-μm-diameter fishing line (Sunstar Co. Ltd., Shanghai, China) and used to press holes at locations (1-2) immediately above the water level and opposite of each other. The tube was then emptied. Next, the line was pulled through using the needle so that it spanned the tube. One end was then secured with waterproof adhesive. Upon setting, the line was pulled taut, and the other end likewise secured. This process was repeated for a second hole pair (3-4) at a second water level. The fishing line ends may be trimmed if desired. The construction process is illustrated in Fig. 4.

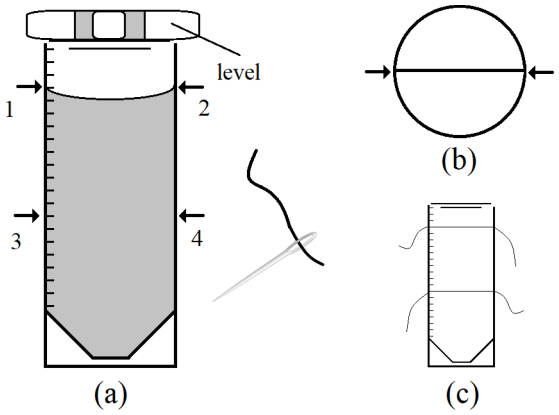

Fig. 4. Procedure for constructing a line target test tube. The test tube is maintained vertical at all times with the use of a level. (a) Water is used to provide reference heights where pairs of holes (1-2, 3-4) are pressed and fishing line is secured with waterproof adhesive. (b) Holes are pressed such that they are opposite to each other and all lie in the same plane. Lines connecting each pair of holes would pass through the tube center, as shown in this top view. (c) Side view of the finished target test tube.

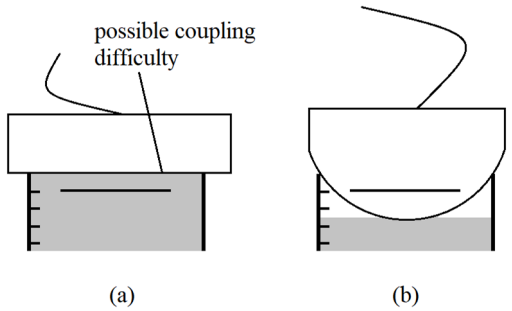

Fig. 5. Coupling for transducers larger than the test tube diameter. (a) Using a straight linear transducer may produce coupling difficulty. (b) Curvilinear transducer, shown exaggerated, can more readily maintain partial contact with the liquid present and thereby avoid coupling difficulty.

2) Imaging Technique: Line target distances were measured as follows. An ultrasonic imaging system XK/21355 (Sichuan Xukang Medical Electrical Appliances Co., Ltd, Chengdu, China) was used to acquire all images using a curvilinear IPX 7 transducer operating at 6.5 MHz. The use of a curvilinear transducer rather than a straight linear transducer minimizes the difficulty in transducer coupling when the lateral dimension of the transducer exceeds the test tube diameter, as illustrated in Fig. 5. For a straight linear transducer, a liquid needs to fill the tube almost entirely to establish contact with the transducer surface. A curvilinear transducer allows the measurement to be made with less than perfect filling. Here, only the center part of the transducer is in contact with the liquid, and therefore, the transducer is only coupled at the center. However, that coupled area is sufficient to perform the sound speed measurements described.

Images were acquired of liquids and agarose gel, as previously described. The acquired images were transferred to a computer. The parallel nature of the line targets was visually verified. Image distances $d_2' - d_1'$ were measured by image examination with Microsoft Windows Paint by examining a line through the image center, as indicated

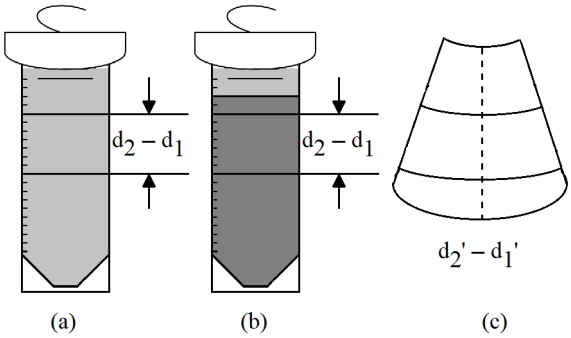

Fig. 6. Image acquisition. (a) Liquids and (b) agarose gel had images obtained with the transducer. The actual line separation $d_2 - d_1$ is contrasted with their apparent distances $d_2' - d_1'$ (c), which were measured through image examination by computer through the centerline.

in Fig. 6. The actual distance $d_2 - d_1$ for the constructed test tube was found by measuring a saline solution with a known sound speed $c_0 = 1540$ m/s in the test tube calibration process.

Image distances, or equivalently apparent distances, were measured as follows using Windows Paint. First, the vertical distance markers were identified. Pixel coordinate values (x_1, y_1) and (x_2, y_2) of the markers corresponding to the greatest and least distances from the transducer were recorded by placing the cursor onto the markers. Calculating $(y_1 - y_2)$/the vertical distance provides the conversion factor (in pixels/cm) between pixels and distances. Likewise, examination of the pixel values of the centerline between the two line targets provides a pixel difference that is then converted to a distance. The points used for the distance measurement were selected from the middle of each line target since targets appeared with some thickness. Distances measured would be located along the same beam provided that x_1 is approximately equal to x_2. The measurement process is depicted in Fig. 7.

3) Saline Solutions: An empirical formula has been previously reported that provides the sound speed of aqueous sodium chloride solutions as a function of salinity and temperature [24]. The formula is

$$c(S, T) = a_0(T) + a_1(T)S \tag{2}$$

with constants a_0 and a_1 given by

$$\begin{aligned} a_0(T) &= 1403.09 + 4.68391\ T - 0.00405388T^2 \\ &\quad + (1.2955 \times 10^{-5})T^3 + (6.914851 \times 10^{-7})T^4 \\ a_1(T) &= 14.019 - 0.114996T + (2.23748 \times 10^{-5})T^2 \\ &\quad + (1.48238 \times 10^{-5})T^3 - (9.46165 \times 10^{-8})T^4 \end{aligned}$$

where S denotes salinity in % (1% is 1 g NaCl dissolved in 100 g solution) and T the Celsius temperature.

This relationship provides a convenient means of calibrating the dual-line target test tube constructed. One first computes the concentration of salt needed to make a solution with sound speed $c = c_0 = 1540$ m/s for the given solution temperature. Using that solution, images of the test tube provide the actual separation $d_2 - d_1$ of the line targets. This value of $d_2 - d_1$ is then used repeatedly for all measurements made with that test tube.

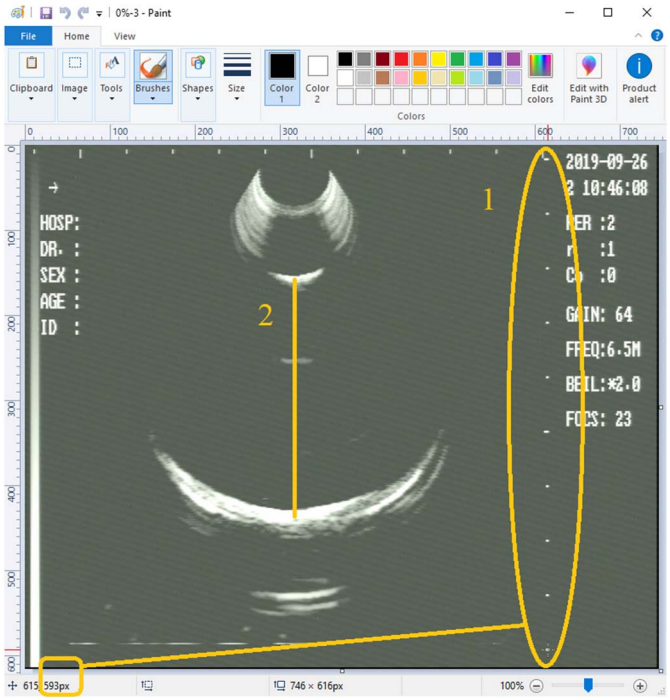

Fig. 7. Distance measurements. In this example, the distance of 9 cm corresponds to a pixel value (x_1, y_1) of (615, 593). The pixel value for the 0 cm distance is likewise obtained, which is then used to calculate the conversion factor. Next, the centerline pixel difference is likewise identified and converted to an image distance $d_2' - d_1'$. Shown is an image acquired for the case of fresh water.

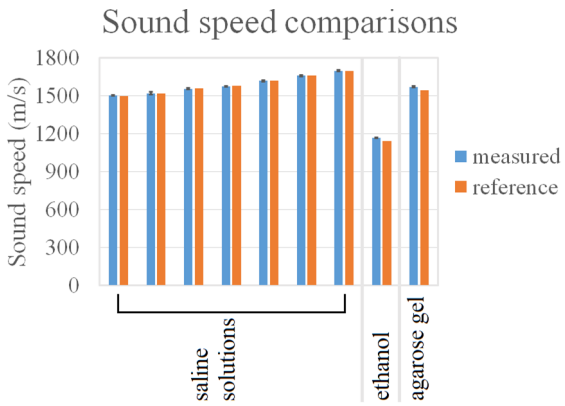

Fig. 8. Comparisons between the measured and reference values. Saline solutions from left to right have reference values of 1501, 1520, 1560, 1580, 1620, 1660, and 1700 m/s. Ethanol and agarose gel have reference speeds of 1144 [25] and 1543 m/s [8], respectively. Error bars denote ±1 standard deviation. Measured values closely match reference values.

This relationship also means that saline solutions provide convenient test solutions. A series of seven solutions were prepared with known sound speeds ranging from 1501 to 1700 m/s to verify the method validity over a range of values. Images of the test tube were obtained ($n = 5$) for each solution to assess experimental variability.

4) Additional Measurements: The variability in sound speed measurements obtained from a single image due to observer variability was examined. Repeated ($n = 5$) measurements of the apparent distance between the two line targets were made for a single image and the corresponding sound speeds were recorded. Their standard deviation was calculated.

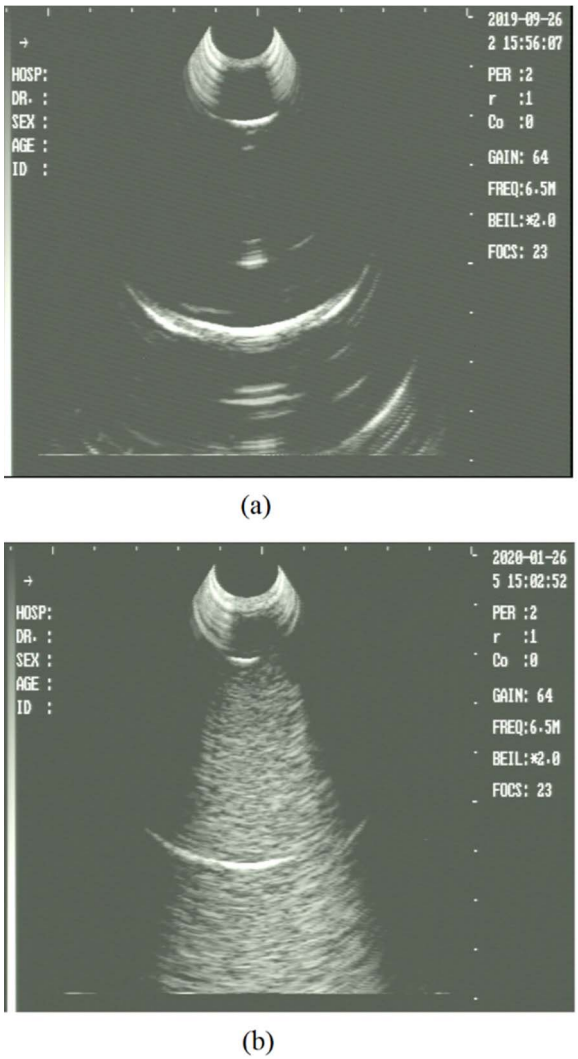

Fig. 9. Ultrasound B-mode images of the measurement process. (a) Image used to calibrate the test tube by measuring the actual distance $d_2 - d_1$. (b) Representative image of the agarose gel cast within the test tube.

Pure ethanol (Shimakyu's Pure Chemicals, Osaka, Japan) was measured to examine a liquid with a lower sound speed than 1501 m/s. Ethanol has a reference sound speed of 1144 m/s [25]. To test the method on a solid phantom material, a solid agarose-based tissue-mimicking gel [8] was cast into the test tube with embedded glass beads (at 8 g/L concentration) to provide ultrasonic backscatter comparable to the actual tissues. The phantom material was measured using water as the coupling agent. A series of images ($n = 5$) were made for each case.

III. Results

A. Test Tube Calibration

The dual-line target test tube that was constructed had the distance between its line targets measured by having a saline solution with sound speed $c = c_0 = 1540$ m/s added and imaged ($n = 5$). The distance was 4.2427 ± 0.0287 cm (mean $\pm$ standard deviation) $= 4.24$ cm. The mathematical average calibration value (4.2427 cm) was used as the value of the actual distance difference $d_2 - d_1$ for all subsequent

TABLE II
COMPARISON OF METHODS

Substance being measured	% Error [a]	Source
distilled water at 19 °C	0.068%	[12]
0.9% saline	0	[12]
distilled water from ~23-40 °C	0.1%	[17]
tissue-mimicking agarose gel	0.04% [b]	[8], [26]
water (reference 1501 m/s)	0.2%	
saline (reference 1520, 1560, 1580, 1620, 1660, 1700 m/s)	0.51%	
ethanol and agarose gel	1.9%	

[a]abs(100(measured – reference))/reference
[b]This figure is based on the reported uncertainty of 0.6 m/s and the reported value of c = 1543 m/s.

measurements. Were a different test tube to be constructed, the calibration process would be expected to measure a different value of $d_2 - d_1$ to be used in making sound speed measurements. Assuming normally distributed errors, the 95% prediction interval, or the range in which 95% of single measurements are expected to fall, was 4.24 cm ± 2.05%.

B. Sound Speed Measurements

The results of sound speed measurements are plotted in Fig. 8. The absolute average percent error (100*abs(mean of measurements − reference value)/reference value) across all measured samples was 0.51%. Across saline solutions only, the value was 0.21%. For ethanol and agarose gel, the error value was 1.9%. Measurements were readily repeatable, with an average standard deviation of 0.34%. No individual measurement had an error exceeding 2.4%. The intra-image standard deviation, arising from observer variability, was 0.39%. The minimum resolvable sound speed difference was approximately 19 m/s.

Representative B-mode images obtained are provided in Fig. 9. For liquids, the line targets are readily identified by 1) looking for the strongest echoes that are 2) located near the approximate physical distances from the transducer face. For the agarose gel, which had glass beads embedded to simulate tissue scatter, the targets nevertheless remain visible and are readily apparent.

IV. DISCUSSION AND CONCLUSION

Sound speed is a crucial material property in ultrasonic studies and is an important parameter to be measured and adjusted in the development of various phantom materials. Although other techniques for measuring sound speed are available, they require specialized setups and expensive equipment that may not be readily obtained. The development of this simple method to measure sound speed avoids the need for such, with the only piece of relatively sophisticated equipment being a simple B-mode ultrasonic imager, which is readily available in medical clinics and laboratories. The imager does not require any specialized modification such as individual scan line data readouts; any commercial imager capable of exporting obtained images may be used. It avoids the need for a large water bath in which samples are suspended.

This method has been shown to reasonably accurately measure (average error 0.51%, maximum observed single measurement error 2.4%) sound speed in both liquids and a tissue-mimicking gel with embedded scatterers. Once any particular test tube is constructed and calibrated, it may be reused indefinitely without further calibration. Provided that one is capable of manually identifying the line targets in the B-mode images, apparent distances are readily examined on a computer using any graphics application. The material sound speed is then computed based on the apparent and actual line target distances. It is possible to process the images automatically using various segmentation techniques. However, to do so would add complexity to the measurement process.

A comparison of the accuracy of this method to previously reported methods is provided in Table II. While this method has larger errors than other methods, it has the advantage of simplicity and ease of use. It can be used with any B-mode scanner and transducer. Any test tube can have two parallel line targets inserted. Errors can be minimized by maximizing the separation d between the lines, and by minimizing Δd and r. Besides these geometric approaches, errors may also be minimized using transducers with shorter pulse lengths. Since images are known to become increasingly blurred [2] as the medium sound speed departs from $c_0 = 1540$ m/s, measurement accuracy likewise is expected to be reduced for large values of Δc from the blurring of target lines.

The measurement technique presented can be readily performed using an A-mode ultrasound system. A-mode systems are simpler than B-mode systems. Pulse arrival times, which are readily measured, correspond to target distances. An A-mode system would not have image blurring effects arising from sound speeds differing from the assumed value of c_0. A-mode systems are not as ubiquitous as B-mode systems, however. A conventional B-mode system can be used to perform various imaging tasks in a laboratory or clinic, with the measurement of sound speed being only one of them.

It is anticipated that this method may be used in the further development of various doped phantoms. For instance, phantoms may be altered with different additives to provide additional functionalities such as temperature sensitivity. To what extent do various additives at various concentrations change their sound speed? Is sound speed altered with temperature changes? Also, this method could be used to conduct studies on various cell suspensions, as well as studies on suspensions of micro- and nanoparticles. For smaller sample volumes, measurements may be performed by combining smaller physical transducers with smaller test tubes.

The main limitation of this method is that it is restricted to liquids, suspensions, and solids that can be cast into a test tube. A piece of solid material can have lines embedded within it; however, unless one has a separate means of obtaining their actual separation distance, one cannot determine the sound speed of the solid material. The agarose gel phantom material is readily produced by combining its components within the test tube itself and allowing the material to cool and solidify.

Many other phantom materials can be similarly produced and measured. Solids that can be melted and poured into the test tube may likewise be measured, provided that melting and subsequent solidification do not alter its sound speed.

In summary, we have developed a simple method to readily and accurately measure sound speeds of liquids, suspensions, and castable solids with only a B-mode imager and minimal additional equipment. It is based on the measurement and comparison of the apparent and actual distances between a pair of line targets.

REFERENCES

[1] M. K. Feldman, S. Katyal, and M. S. Blackwood, "US artifacts," *RadioGraphics*, vol. 29, no. 4, pp. 1179–1189, Jul. 2009, doi: 10.1148/rg.294085199.

[2] N. J. Dudley, N. M. Gibson, M. J. Fleckney, and P. D. Clark, "The effect of speed of sound in ultrasound test objects on lateral resolution," *Ultrasound Med. Biol.*, vol. 28, nos. 11–12, pp. 1561–1564, Nov./Dec. 2002, doi: 10.1016/S0301-5629(02)00648-8.

[3] K. W. Cushing, F. Garofalo, C. Magnusson, L. Ekblad, H. Bruus, and T. Laurell, "Ultrasound characterization of microbead and cell suspensions by speed of sound measurements of neutrally buoyant samples," *Anal. Chem.*, vol. 89, no. 17, pp. 8917–8923, Sep. 2017, doi: 10.1021/acs.analchem.7b01388.

[4] E. Hincapié Gómez, J. Tryner, A. J. Aligata, J. C. Quinn, and A. J. Marchese, "Measurement of acoustic properties of microalgae and implications for the performance of ultrasonic harvesting systems," *Algal Res.*, vol. 31, pp. 77–86, Apr. 2018, doi: 10.1016/j.algal.2018.01.015.

[5] B. Mahmoud, H. P. Rice, L. Mortimer, M. Fairweather, J. Peakall, and D. Harbottle, "Acoustic method for determination of the thermal properties of nanofluids," *Ind. Eng. Chem. Res.*, vol. 58, no. 42, pp. 19719–19731, Oct. 2019, doi: 10.1021/acs.iecr.9b02983.

[6] M. T. Zafarani-Moattar and R. Majdan-Cegincara, "Effect of temperature on volumetric and transport properties of nanofluids containing ZnO nanoparticles poly(ethylene glycol) and water," *J. Chem. Thermodyn.*, vol. 54, pp. 55–67, Nov. 2012, doi: 10.1016/j.jct.2012.03.010.

[7] M. J. W. Povey, "Ultrasound particle sizing: A review," *Particuology*, vol. 11, no. 2, pp. 135–147, Apr. 2013, doi: 10.1016/j.partic.2012.05.010.

[8] E. L. Madsen, G. R. Frank, and F. Dong, "Liquid or solid ultrasonically tissue-mimicking materials with very low scatter," *Ultrasound Med. Biol.*, vol. 24, no. 4, pp. 535–542, 1998, doi: 10.1016/S0301-5629(98)00013-1.

[9] K. Takegami, Y. Kaneko, T. Watanabe, T. Maruyama, Y. Matsumoto, and H. Nagawa, "Polyacrylamide gel containing egg white as new model for irradiation experiments using focused ultrasound," *Ultrasound Med. Biol.*, vol. 30, no. 10, pp. 1419–1422, Oct. 2004, doi: 10.1016/j.ultrasmedbio.2004.07.016.

[10] A. Cafarelli, P. Miloro, A. Verbeni, M. Carbone, and A. Menciassi, "Speed of sound in rubber-based materials for ultrasonic phantoms," *J. Ultrasound*, vol. 19, no. 4, pp. 251–256, Dec. 2016, doi: 10.1007/s40477-016-0204-7.

[11] J. R. Pellam and J. K. Galt, "Ultrasonic propagation in liquids: I. Application of pulse technique to velocity and absorption measurements at 15 megacycles," *J. Chem. Phys.*, vol. 14, no. 10, pp. 608–614, Oct. 1946, doi: 10.1063/1.1724072.

[12] I. Y. Kuo, B. Hete, and K. K. Shung, "A novel method for the measurement of acoustic speed," *J. Acoust. Soc. Amer.*, vol. 88, no. 4, pp. 1679–1682, Oct. 1990, doi: 10.1121/1.400242.

[13] F. Bakkali *et al.*, "Ultrasonic measurement of milk coagulation time," *Meas. Sci. Technol.*, vol. 12, no. 12, pp. 2154–2159, Dec. 2001, doi: 10.1088/0957-0233/12/12/317.

[14] A. Leydier, J. Mathieu, and G. Despaux, "The two coupling fluids method for ultrasonic velocity measurement. Application to biological tissues," *Meas. Sci. Technol.*, vol. 20, no. 9, Sep. 2009, Art. no. 095801, doi: 10.1088/0957-0233/20/9/095801.

[15] J. Ophir and T. Lin, "A calibration-free method for measurement of sound speed in biological tissue samples," *IEEE Trans. Ultrason., Ferroelectr., Freq. Control*, vol. 35, no. 5, pp. 573–577, Sep. 1988, doi: 10.1109/58.8035.

[16] D. A. Çelik *et al.*, "Design and implementation of an ultrasonic sensor for rapid monitoring of industrial malolactic fermentation of wines," *Instrum. Sci. Technol.*, vol. 46, no. 4, pp. 387–407, Jul. 2018, doi: 10.1080/10739149.2017.1394878.

[17] L. Elvira, C. Durán, C. Sierra, P. Resa, and F. M. D. Espinosa, "Ultrasonic measurement device for the characterization of microbiological and biochemical processes in liquid media," *Meas. Sci. Technol.*, vol. 18, no. 7, pp. 2189–2196, Jul. 2007, doi: 10.1088/0957-0233/18/7/051.

[18] P. V. Nelson, M. J. W. Povey, and Y. Wang, "An ultrasound velocity and attenuation scanner for viewing the temporal evolution of a dispersed phase in fluids," *Rev. Sci. Instrum.*, vol. 72, no. 11, pp. 4234–4241, Nov. 2001, doi: 10.1063/1.1408936.

[19] F. Piscaglia, C. F. Dietrich, C. Nolsoe, O. H. Giljia, and D. Gaitini, "Birth of 'echoscopy'—The EFSUMB point view," *Ultraschall Med.*, vol. 34, no. 1, p. 92, Feb. 2013, doi: 10.1055/s-0032-1319207.

[20] T. L. A. van den Heuvel, D. J. Graham, K. J. Smith, C. L. de Korte, and J. A. Neasham, "Development of a low-cost medical ultrasound scanner using a monostatic synthetic aperture," *IEEE Trans. Biomed. Circuits Syst.*, vol. 11, no. 4, pp. 849–857, Aug. 2017, doi: 10.1109/TBCAS.2017.2695240.

[21] T. L. A. van den Heuvel, D. de Bruijn, D. Moens-van de Moesdijk, A. Beverdam, B. van Ginneken, and C. L. de Korte, "Comparison study of low-cost ultrasound devices for estimation of gestational age in resource-limited countries," *Ultrasound Med. Biol.*, vol. 44, no. 11, pp. 2250–2260, Nov. 2018, doi: 10.1016/j.ultrasmedbio.2018.05.023.

[22] K. Thayalan, "Ultrasound imaging," in *Basic Radiological Physics*, 2nd ed. New Delhi, India: The Health Sci., 2017, p. 252.

[23] J. Semmlow, "Noise," in *Signals and Systems for Bioengineers*, 2nd ed. Waltham, MA, USA: Academic, 2012, p. 16.

[24] S. J. Kleiss and L. A. Sanchez, "Dependence of speed of sound on salinity and temperature in concentrated NaCl solutions," *Sol. Energy*, vol. 45, no. 4, pp. 201–206, 1990, doi: 10.1016/0038-092X(90)90087-S.

[25] (2004). *Velocity of Sound in common Liquids*. Engineering ToolBox. [Online]. Available: https://www.engineeringtoolbox.com/sound-speed-liquids-d_715.html

[26] E. L. Madsen, J. A. Zagzebski, and G. R. Frank, "Oil-in-gelatin dispersions for use as ultrasonically tissue-mimicking materials," *Ultrasound Med. Biol.*, vol. 8, no. 3, pp. 277–287, Jan. 1982.

Wanwei Yu is currently pursuing the master's degree with the Institute of Biomedical Engineering, National Chiao Tung University, Hsinchu, Taiwan.

Her research interests include developing new techniques for measuring various constants of ultrasonically relevant materials.

Nelson G. Chen was born in Knoxville, TN, USA, in 1977. He received the B.S. degree in engineering science from the University of Tennessee, Knoxville, in 1999, and the M.S. and Ph.D. degrees in biomedical engineering from the University of Michigan, Ann Arbor, MI, USA, in 2001 and 2009, respectively.

From 2008 to 2013, he was a Research Scientist at Sci-Tec, Inc. Since then, he has been an Assistant Professor at National Chiao Tung University, Hsinchu, Taiwan, where he heads the Applied Ultrasound Laboratory, Department of Electrical and Computer Engineering. His research interests mainly include the interaction of ultrasound with various suspended particles and associated bioeffects and their measurement. Secondary interests are the study of chemical fingerprints and their properties and applications.

Dr. Chen received the University Superior Mentorship Award in 2019.